


RESEARCH ARTICLE

Single-level cervical disc arthroplasty in the spine with reversible kyphosis: A finite element study

Xu Hu^{1,2} | Majiao Jiang³ | Ying Hong³ | Xin Rong¹ | Kangkang Huang¹ | Hao Liu¹ | Dan Pu⁴ | Beiyu Wang¹ 

¹Department of Orthopedics, Orthopedic Research Institute, West China Hospital, Sichuan University, Chengdu, Sichuan Province, China

²Department of Biomedical Engineering, City University of Hong Kong, Hong Kong SAR, China

³Department of Anesthesia and Operation Center, West China School of Nursing, West China Hospital, Sichuan University, Chengdu, Sichuan Province, China

⁴Clinic Skill Center, West China Hospital, Sichuan University, Chengdu, Sichuan, China

Correspondence

Beiyu Wang, Department of Orthopedics, Orthopedic Research Institute, West China Hospital, Sichuan University, 37 Guoxue Lane, Chengdu, Sichuan Province 610041, China. Email: dove-baker@163.com

Funding information

1:3:5 project for disciplines of excellence - Clinical Research Incubation Project, West China Hospital, Sichuan University, Grant/Award Number: 2019HXFH040; Chengdu Science and Technology Program Projects, Grant/Award Number: 2017-CY02-00025-GX; National Natural Science Foundation of China, Grant/Award Number: 81902190; The Science And Technology Project of The Health Planning Committee of Sichuan, Grant/Award Number: 21PJ039; Key Research and Development Project of Science and Technology Department of Sichuan Province, Grant/Award Number: 2020YFS0084

Abstract

Background: Our previous studies found the single-level cervical disc arthroplasty (CDA) might be a feasible treatment for the patients with reversible kyphosis (RK). Theoretically, the change of cervical alignment from lordosis to RK comes with the biomechanical alteration of prostheses and cervical spine. However, the biomechanical data of CDA in the spine with RK have not been reported. This study aimed at establishing finite element (FE) models to (1) explore the effects of RK on the biomechanics of artificial cervical disc; (2) investigate the biomechanical differences of single-level anterior cervical discectomy and fusion (ACDF) and CDA in the cervical spine with RK.

Methods: The FE models of the cervical spine with lordosis and RK were constructed, then three single-level surgical models were developed: (1) RK + ACDF; (2) RK + CDA; (3) lordosis + CDA. A 73.6-N follower load combined with 1 N·m moment was applied at the C2 vertebra to produce cervical motion.

Results: At the surgical level, “lordosis + CDA” had the greatest ROM (except for flexion) while “RK + ACDF” had the minimum ROM. However, at adjacent levels, the ROM of “RK + ACDF” increased by 4.05% to 38.04% in comparison to “RK + CDA.” “RK + ACDF” had the greatest prosthesis interface stress, while the maximum prosthesis interface stress of “RK + CDA” was at least 2.15 times higher than “lordosis + CDA.” Similarly, “RK + ACDF” had the greatest intradiscal pressure (IDP) at adjacent levels, while the IDP of “RK + CDA” was 1.6 to 6.7 times higher than “lordosis + CDA.” At the surgical level, “RK + CDA” had the greatest facet joint stress (except for extension), which was 1.9 to 11.2 times higher than “lordosis + CDA.” At the adjacent levels, “RK + CDA” had the greatest facet joint stress (except for extension), followed by “RK + ACDF” and “lordosis + CDA” in descending order.

Conclusions: RK significantly changed the biomechanics of CDA, which is demonstrated by the decreased ROM and the significantly increased prosthesis interface stress, IDP, and facet joint stress in the “RK + CDA” model. Compared with ACDF,

Xu Hu and Majiao Jiang have contributed equally to this work and share the first authorship.

This is an open access article under the terms of the [Creative Commons Attribution-NonCommercial-NoDerivs](https://creativecommons.org/licenses/by-nc-nd/4.0/) License, which permits use and distribution in any medium, provided the original work is properly cited, the use is non-commercial and no modifications or adaptations are made.

© 2022 The Authors. *JOR Spine* published by Wiley Periodicals LLC on behalf of Orthopaedic Research Society.

CDA overall exhibited a better biomechanical performance in the cervical spine with RK, with the increased ROM of surgical level and facet joint stress and the decreased ROM of adjacent levels, prosthesis interface stress, and IDP.

KEYWORDS

anterior cervical discectomy and fusion, biomechanics, cervical disc arthroplasty, finite element analysis, reversible kyphosis

1 | INTRODUCTION

Anterior cervical discectomy fusion (ACDF) is the standard procedure for managing symptomatic cervical degenerative disc disease that did not respond to conservative treatment. However, by converting a mobile, functional spinal unit into a fixed segment, ACDF resulted in the increased strain at adjacent levels, presumably leading to accelerated disc degeneration and/or segmental instability at these levels.^{1,2} In response to these concerns, cervical disc arthroplasty (CDA) has emerged as an alternative to fusion, aiming to restore normal intervertebral motion and avoid the abnormal kinematic stresses produced by fusion.³ Several meta-analyses and randomized controlled studies with long-term follow-up have revealed that CDA could achieve comparable or superior clinical and radiological outcomes compared with ACDF.⁴⁻⁶

The lordosis has been extensively considered as the normal and physiological curvature of cervical spine, but the kyphosis, which is regarded as the abnormal deformity or morbid status, accounted for up to 35% asymptomatic population.^{7,8} In a study of 958 asymptomatic adult volunteers, Kim et al. reported that more than one-fourth of the participants (26.3%) had kyphotic cervical posture, and almost five-sixth of the kyphotic individuals (83.3%) exhibited reversible kyphosis (RK).⁹

There was no consensus about whether CDA could be indicated for the patients with kyphosis. Due to the strict indications of CDA, the lack of anterior column support for most artificial cervical disc prostheses, and reasonable prudence toward this new surgical technique, most studies reported the application of CDA in the cervical spine with lordosis.^{5,6,10} Some surgeons regarded kyphosis or severe kyphosis as a contraindication for CDA,¹¹⁻¹³ given that the segmental kyphosis was massively reported after the insertion of BRYAN® Cervical Disc (Medtronic Sofamor Danek).¹⁴ But some authors found that CDA could restore the cervical alignment to some extent.¹⁵⁻¹⁸ Our previous studies^{8,19} also found that for the single-level CDA patients, both lordosis and RK groups achieved satisfactory and comparable clinical outcomes; in the patients with RK, the clinical and radiological outcomes of CDA were non-inferior to those of ACDF.

Biomechanically, a lordotic configuration could effectively resist compressive loads and minimize the stress on the vertebral body endplates.⁷ Also, the lordotic shape allows the cervical spine to distribute nearly 64% load of the head through the posterior columns and 36% load through the anterior column.²⁰ It is predicted that the change of cervical alignment from lordosis to RK comes with the

biomechanical alteration of prostheses and cervical spine. However, the biomechanical data of CDA in the spine with RK have not been reported.

The purpose of this study was to (1) establish finite element (FE) models to simulate three single-level operations, namely “RK + ACDF,” “RK + CDA,” and “lordosis + CDA”; (2) explore the effects of RK on the biomechanics of artificial cervical disc and cervical spine by comparing the FE analysis results of “RK + CDA” and “lordosis + CDA”; (3) investigate the biomechanical differences of single-level ACDF and CDA in the cervical spine with RK by comparing the FE analysis results of “RK + ACDF” and “RK + CDA.”

2 | MATERIALS AND METHODS

2.1 | Construction of cervical spine model with lordosis and RK

The nonlinear FE model of the cervical spine with lordosis (C2–C7) was developed and validated in our previous study.²¹ This lordosis model was constructed based on the computed tomography (CT) images of a young male without cervical degeneration (28-year-old, 165 cm, 65 kg) with a resolution of 0.75 mm and an interval of 0.69 mm (SOMATOM Definition AS+, Siemens). Similarly, the CT images of an asymptomatic male with RK (32-year-old, 161 cm, 62 kg) were adopted to establish the RK model (Figure 1). The RK was defined when the kyphosis in the neutral position was spontaneously corrected to straight or lordosis in extension.^{8,19}

The CT images (Digital Imaging and Communications, DICOM format) were imported into Mimics 17.0 (Materialize Inc.) to reconstruct the geometric structure of the C2–C7 cervical vertebrae. Then, the reconstructed model was imported into Geomagic Studio 12.0 (3D System Corporation) to acquire nonuniform rational B-splines surfaces. In this step, the errors and regional burrs of model were corrected by denoising, surfacing, and smoothing; the cortical and cancellous bones were reconstructed individually to achieve an accurate anatomic model. Next, the model was imported into Hypermesh 12.0 (Altair) to generate a high-quality FE mesh. The material property and element types were listed in Table 1. The number of elements and nodes of each model were presented in Table 2. The mesh convergence of a FE model was tested and verified by comparing the Von Mises stress in different mesh resolutions. The mesh was considered converged if the Von Mises stress changed less than 5% when the

FIGURE 1 The finite element model of reversible kyphosis (RK). The cervical spine model with RK displayed kyphosis in neutral position (A), increased kyphosis in flexion (B), and lordosis in extension (C)

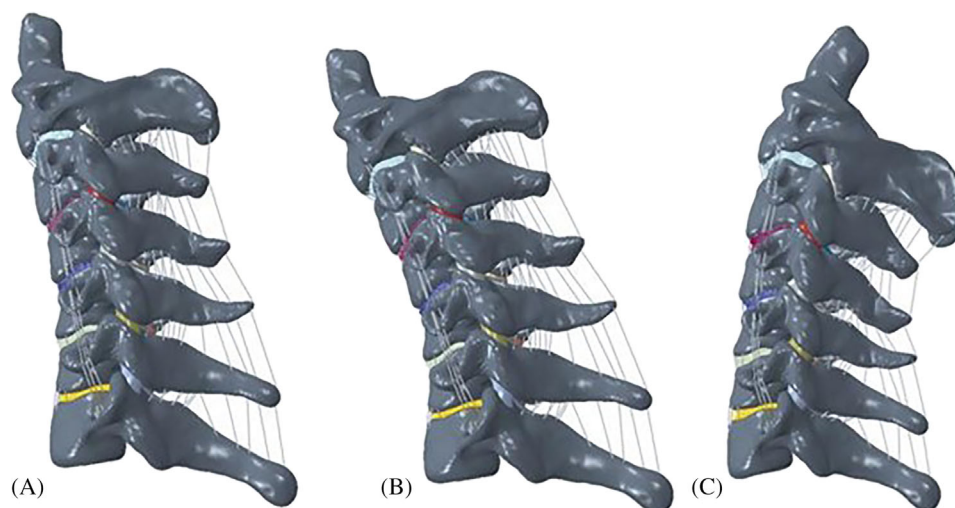


TABLE 1 The material properties and element types of finite element models

	Young's modulus (MPa)	Poisson ratio	Element type	References
Cortical bone	12 000	0.3	C3D10	22,23
Cancellous bone	450	0.25	C3D10	22,24
Cartilage	10.4	0.4	C3D20	21,22
Endplate	500	0.25	C3D20	22,24
Nucleus pulposus	Hyperelastic, Mooney–Rivlin, C1 = 0.12, C2 = 0.03	0.499	C3D20	23,25
Annulus fibrosus substance	Hyperelastic, Mooney–Rivlin, C1 = 0.18, C2 = 0.045	0.45	C3D20	23,25
Annulus fibers	360–550	–	T3D2	26,27
ALL	30	–	T3D2	22,24
PLL	20	–	T3D2	21,22
Ligamentum flavum	1.5	–	T3D2	21,22
Capsular ligament	20	–	T3D2	22,24
Interspinous ligament	1.5	–	T3D2	22,24
Supraspinous ligament	1.5	–	T3D2	21,22
Titanium alloy	110 000	0.3	C3D10	21,22
PEEK	3600	0.3	C3D10	21,24

Abbreviations: ALL, anterior longitudinal ligament; PLL, posterior longitudinal ligament.

mesh density was doubled. The 10-node second-order tetrahedral C3D10 element was used for the components of bone and prostheses; the second-order 20-node hexahedral C3D20 element was used for the components of cartilage and intervertebral disc; the tension-only truss element was used for ligaments and annular fiber. Finally, the model was imported into ABAQUS 6.9.1 (Dassault Systems Corporation) to set boundary conditions and perform the analysis.

The cancellous bone region of each vertebra was set as solid elements. The cortical bone and bony endplates of each vertebra were constructed as a shell with a thickness of 4 mm.²⁸ The intervertebral disc consisted of the annulus fibrosus and nucleus pulposus with a volume ratio of 6:4. The annulus fibers, which accounted for approximately 19% of the entire annulus fibrosus volume, were embedded in the ground substance with an inclination to the transverse plane between 15 and 30 degrees.²⁸ The outer layer of nucleus pulposus and the inner layer of

annulus fibrosus shared the same nodes (Figure 2). A tie connection was defined between the intervertebral disc and endplates. The facet joint space was 0.5 mm, and each facet joint was covered by an articular cartilage layer with nonlinear frictionless surface-to-surface contact.²¹ Five groups of ligaments, namely anterior longitudinal ligament (ALL), posterior longitudinal ligament (PLL), ligamentum flavum, interspinous ligament, and capsular ligament, were attached to the corresponding vertebrae using tension-only truss elements.

2.2 | Construction of prosthesis model

The three-dimensional computer-aided design model of the Zero-P Spacer (Synthes) and Prestige LP Disc (Medtronic Sofamor Danek) were built in this study. According to the measurements of intervertebral

space at C5–C6 level and size parameters of prostheses, the length, width, and height of Prestige LP Disc were 16, 12, and 6 mm; the corresponding data of Zero-P Spacer were 16.5, 17.5, and 6 mm (Figure 3). The ball-and-trough articulation design of Prestige LP Disc allows the flexion-extension motion to be coupled with the anterior–posterior translation in the sagittal plane.²⁹ The Zero-P Spacer consists of PEEK interbody spacer, titanium alloy plate, and screws.

These prostheses were implanted at the C5–C6 level. To simulate the surgical operation, the intervertebral disc, ALL, and PLL of C5–C6 level were completely removed, and the lower endplate of C5 vertebra and the upper endplate of C6 vertebra were partially removed.³⁰ The cancellous bone graft, which was defined as frictionless, filled the middle cage of Zero-P Spacer.²¹ A nonbonded contact was applied between the supra- and infra-adjacent surfaces of the cage and the relevant vertebral surfaces with a contact friction coefficient of 0.3.²¹ The tie constraint was applied to graft-vertebrae and screw-vertebrae interfaces to simulate rigid fusion and sufficient osseointegration.³¹ The implant-implant interfaces of the artificial cervical disc were defined as surface-to-surface sliding contact with a friction coefficient of 0.07.²¹

In total, three surgical procedures were simulated by FE models, that is, “RK + Zero-P Spacer (RK + ACDF),” “RK + Prestige LP Disc (RK + CDA),” and “lordosis + Prestige LP Disc (lordosis + CDA)” (Figure 4).

2.3 | Boundary conditions

The lordosis and RK models were fixed at the inferior endplate of C7 vertebra. The follower loads of 73.6 N were applied at the C2

vertebra to simulate head weight. A 1 N·m moment was applied at the odontoid to produce flexion, extension, lateral bending, and axial rotation. For all models, the following parameters were recorded in six different directions at the surgical level and/or adjacent levels: the range of motion (ROM), intradiscal pressure (IDP, the maximum Von Mises stress of intervertebral disc), facet joint stress (the maximum Von Mises stress of facet joint), and the maximum Von Mises stress of the prosthesis.

3 | RESULTS

3.1 | Validation of the lordosis and RK model

The ROMs of lordosis model were within the one standard deviation of previous experimental data,^{32–34} which indicated that the current lordosis model could statistically represent a healthy individual (Figure 5).

To our knowledge, no in vivo or in vitro cadaver studies reported the ROMs of the cervical spine with kyphosis. This study constructed the FE model of the cervical spine with RK for the first time. This RK model displayed kyphosis in a neutral position, increased kyphosis in flexion, and lordosis in extension, which conformed to the definition of RK (Figure 1). The ROMs of RK model in extension or flexion were similar to the kyphosis model of John et al.³⁵ (Table 3).

3.2 | Range of motion

The ROMs of different models were presented in Figure 6. At C5–C6 level, compared with “RK + CDA,” the ROM of “RK + ACDF” decreased by 86.24%, 64.99%, 66.79%, 67.46%, 67.28%, 70.04% in flexion, extension, left bending, right bending, left rotation, and right rotation, respectively; compared with “lordosis + CDA,” the ROM of “RK + CDA” increased by 14.74% in flexion, but decreased by 58.19%, 5.63%, 10.63%, 4.24%, 9.59% in other directions.

At C4–C5 level, compared with “RK + CDA,” the ROM of “RK + ACDF” increased by 4.80%, 4.05%, 4.52%, 4.47%, 4.67%, 5.60% in flexion, extension, left bending, right bending, left rotation, and right rotation, respectively; compared with “lordosis + CDA,” the ROM of

TABLE 2 The number of elements and nodes of each model

Model	Element	Node
Lordosis	410 564	568 273
Reversible kyphosis	406 871	506 547
Reversible kyphosis + ACDF	586 379	802 101
Reversible kyphosis + CDA	544 515	728 053
Lordosis + CDA	495 197	672 174

Abbreviations: ACDF, anterior cervical discectomy fusion; CDA, cervical disc arthroplasty.

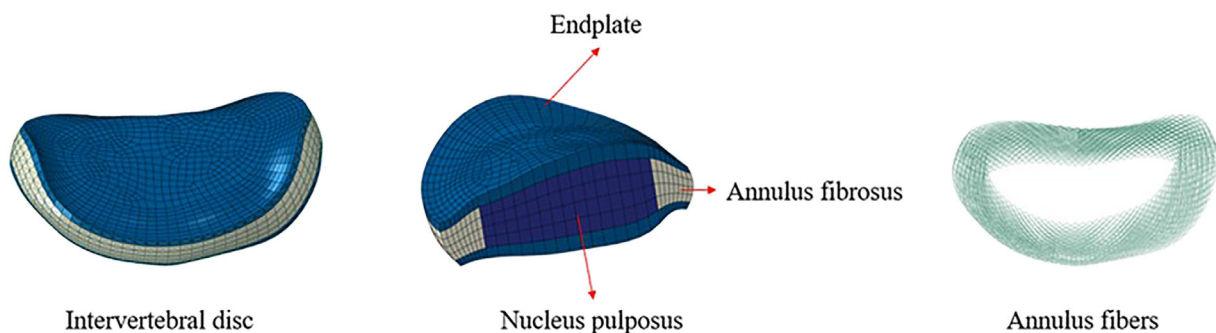


FIGURE 2 The finite element model of the intervertebral disc

FIGURE 3 The finite element models of prostheses. (A) Prestige LP Disc; (B) Zero-P Spacer

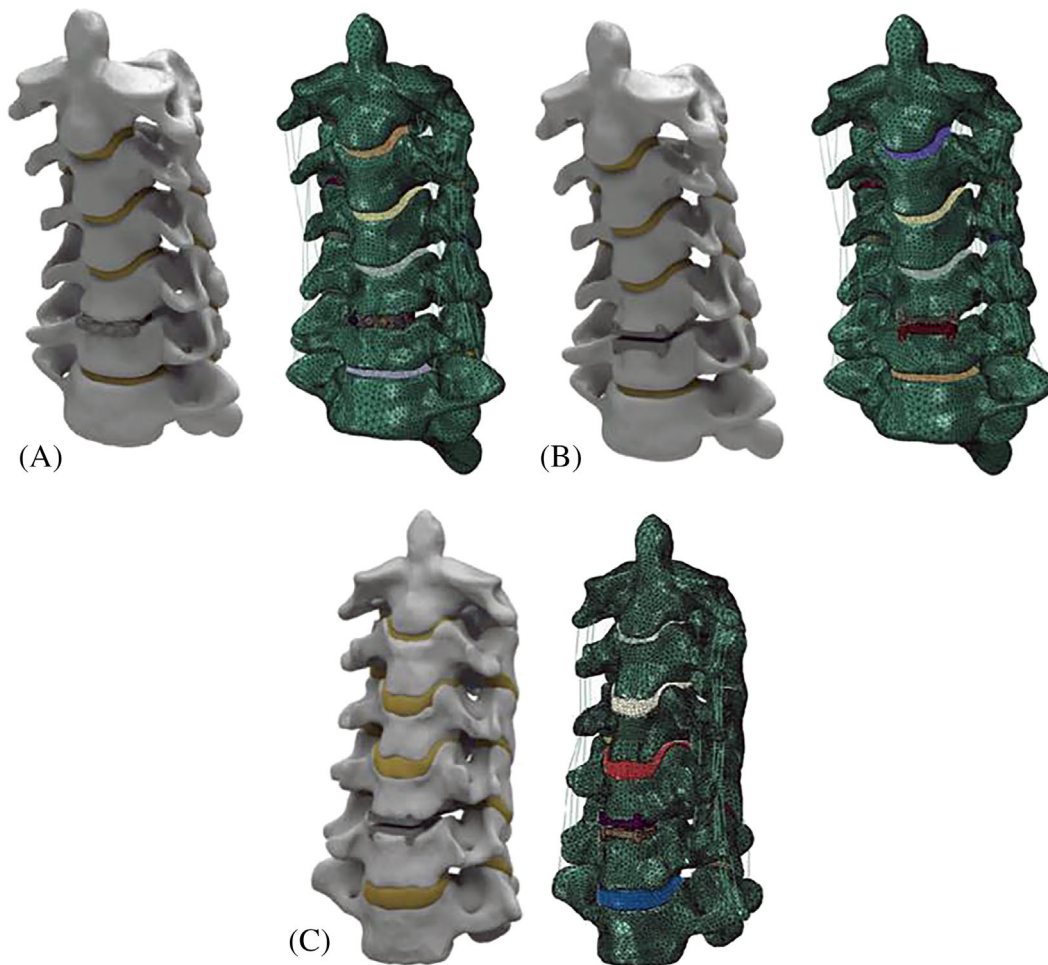
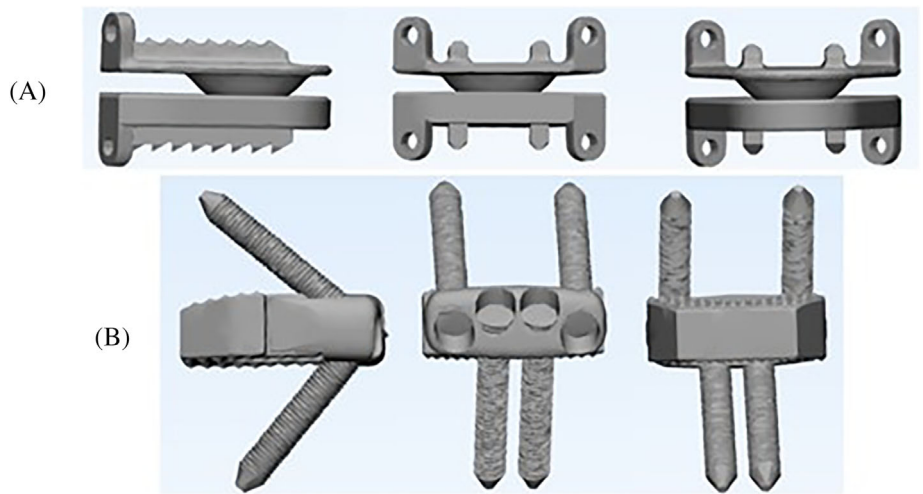


FIGURE 4 Three simulated surgical procedures. (A) Reversible kyphosis + Zero-P Spacer, (B) reversible kyphosis + Prestige-LP Disc, and (C) lordosis + Prestige-LP Disc

“RK + CDA” increased by 79.21% in flexion, but decreased by 55.18%, 2.29%, 3.24%, 3.39%, 3.56% in other directions.

At C6–C7 level, compared with “RK + CDA,” the ROM of “RK + ACDF” increased by 17.16%, 12.90%, 38.04%, 33.35%, 21.19%,

20.78% in flexion, extension, left bending, right bending, left rotation, and right rotation, respectively; compared with “lordosis + CDA,” the ROM of “RK + CDA” increased 53.76% in flexion, but decreased by 54.53%, 15.20%, 16.36%, 10.43%, 11.70% in other directions.

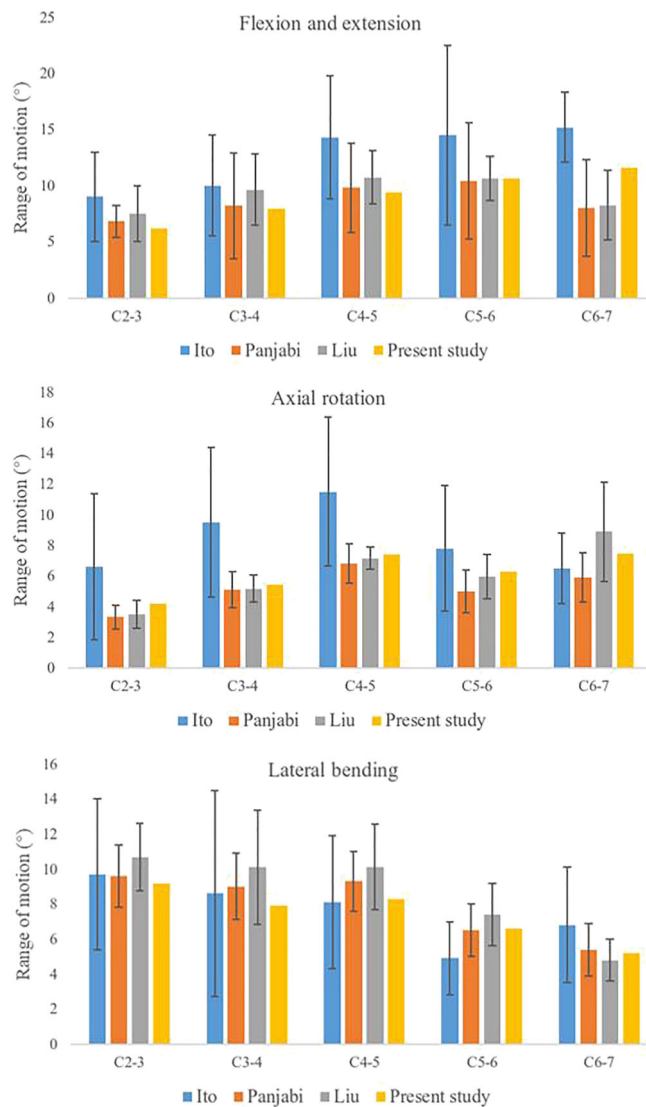


FIGURE 5 The comparison of range of motions between the lordosis model and experimental data

3.3 | The maximum Von Mises stress of the prosthesis

The maximum Von Mises stress of the prosthesis of “RK + CDA” was at least 2.15 times higher than that of “lordosis + CDA”. Compared with “RK + CDA,” the maximum Von Mises stress of the prosthesis of “RK + ACDF” increased by 31.46%, 33.11%, 50.63%, 70.85%, 34.41%, 52.71% in flexion, extension, left bending, right bending, left rotation, and right rotation, respectively (Figure 7). In terms of “RK + ACDF,” the maximum Von Mises stress of the interbody spacer occurred at the anterior part in different directions of movement (Figure 8).

3.4 | IDP at adjacent levels

At C4–C5 level, the IDP of “RK + CDA” was 2.3 to 6.7 times higher than that of “lordosis + CDA”; compared with “RK + CDA,” the IDP

TABLE 3 The comparison of range of motions in flexion or extension between reversible kyphosis model and the kyphosis model of John et al.³⁵

	C2–C3	C3–C4	C4–C5	C5–C6	C6–C7
Flexion					
John et al. ³⁵	3.36°	3.35°	4.77°	4.5°	5.36°
Present study	4.56°	2.88°	3.97°	5.12°	5.94°
Extension					
John et al. ³⁵	3.28°	3.58°	4.99°	3.31°	3.47°
Present study	2.92°	2.14°	2.23°	2.21°	4.17°

of “RK + ACDF” increased by 25.18%, 41.12%, 33.65%, 25.00%, 27.21%, 23.07% in flexion, extension, left bending, right bending, left rotation, and right rotation, respectively (Figure 9).

At C6–C7 level, the IDP of “RK + CDA” was 1.6 to 4.9 times higher than that of “lordosis + CDA”; compared with “RK + CDA,” the IDP of “RK + ACDF” increased by 22.62%, 17.61%, 13.86%, 17.08%, 19.71%, 23.31% in flexion, extension, left bending, right bending, left rotation, and right rotation, respectively (Figure 9).

3.5 | Facet joint stress

The facet joint stress of different models was presented in Figure 10. At C5–C6 level, compared with of RK model, the facet joint stress of “RK + ACDF” decreased by 34.23%, 77.15%, 48.44%, 50.16%, 44.18%, 43.25% in flexion, extension, left bending, right bending, left rotation, and right rotation respectively, while the facet joint stress of “RK + CDA” increased by 47.17%, 2.94%, 15.46%, 35.21%, 28.96%, 20.96% during the same motion. The facet joint stress of “RK + CDA” was 1.9 to 11.2 times higher than that of “lordosis + CDA.”

At C4–C5 level, compared with “RK + ACDF,” the facet joint stress of “RK + CDA” increased by 15.38%, 143.48%, 47.64%, 28.60%, 25.66%, 33.33% in flexion, extension, left bending, right bending, left rotation, and right rotation, respectively; except for extension, the facet joint stress of “RK + CDA” was 1.5 to 10.9 times higher than that of “lordosis + CDA.”

At C6–C7 level, compared with “RK + ACDF,” the facet joint stress of “RK + CDA” increased by 40.84%, 47.93%, 42.41%, 38.93%, 41.80%, 39.05% in flexion, extension, left bending, right bending, left rotation, and right rotation, respectively; except for extension, the facet joint stress of “RK + CDA” was 1.14 to 12.8 times higher than that of “lordosis + CDA.”

4 | DISCUSSION

4.1 | Construction of cervical spine model with RK

At the time of manuscript preparation, the FE model of proximal junctional kyphosis after the surgery for adult spinal deformity (mainly at

FIGURE 6 The comparison of range of motions between different models at surgical and adjacent levels

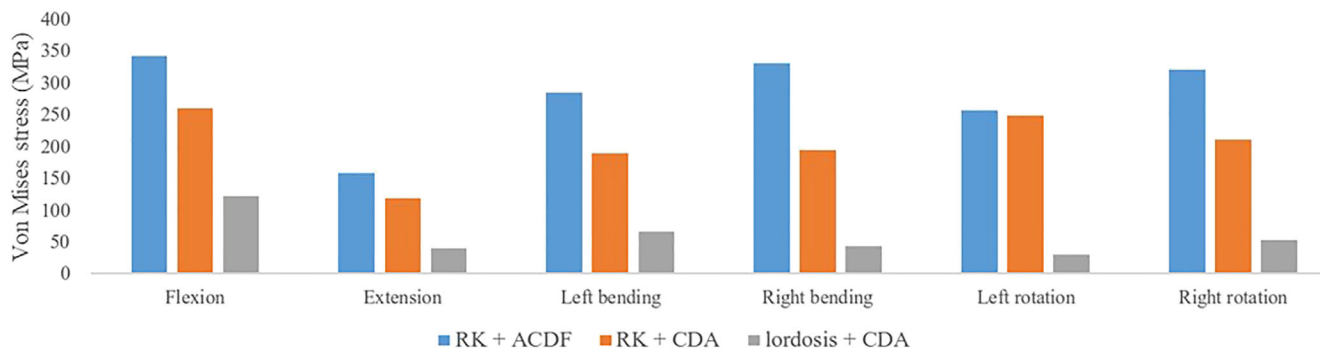
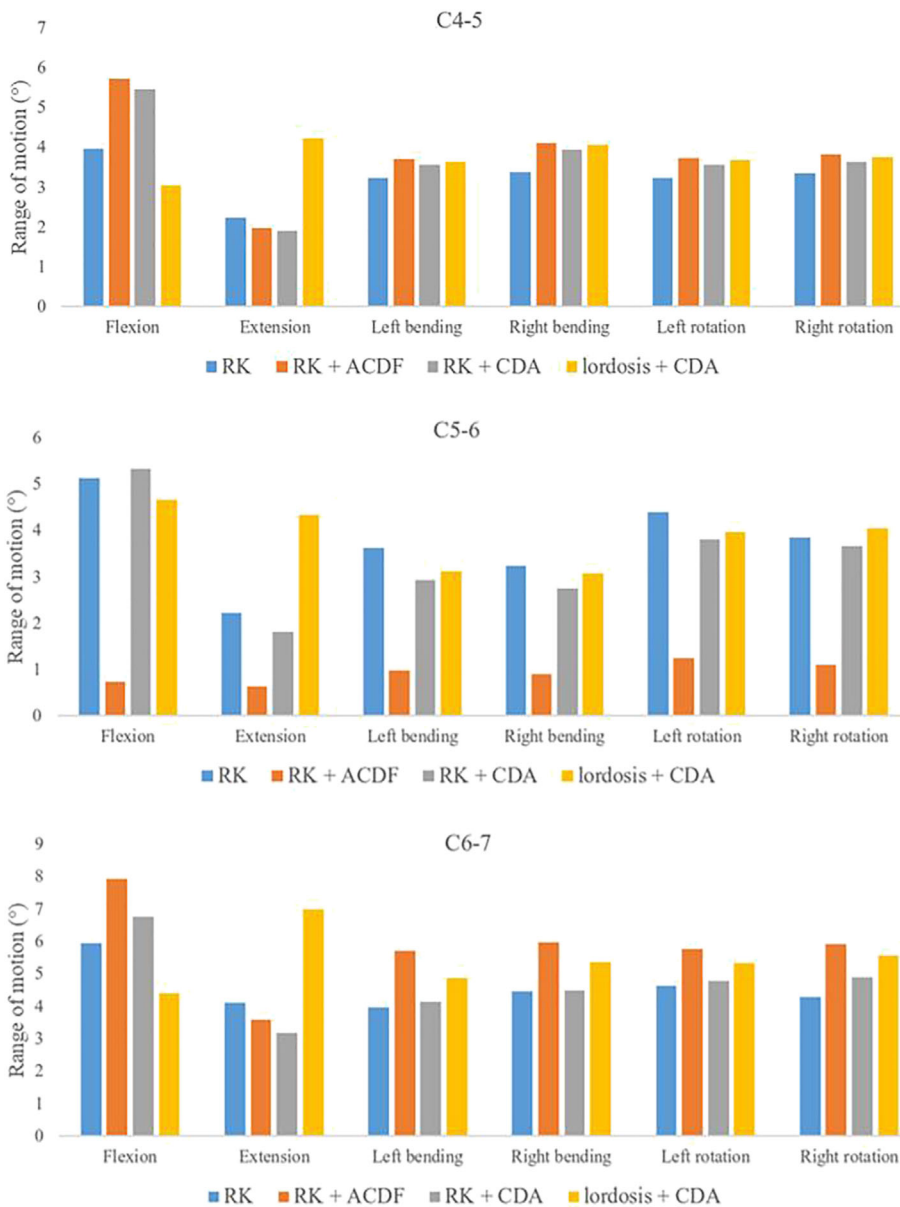


FIGURE 7 The comparison of the maximum Von Mises stress of the prosthesis between different models

the thoracic and lumbar spine) was well-established. However, no in vivo or in vitro cadaver studies reported the ROMs of the cervical spine with kyphosis. Very few FE studies focused on the cervical spine

with malalignment such as straight and kyphosis. Chen et al. compared the strain behavior and ROMs of malaligned cervical spine implanted with different prostheses, but the ROMs of the intact

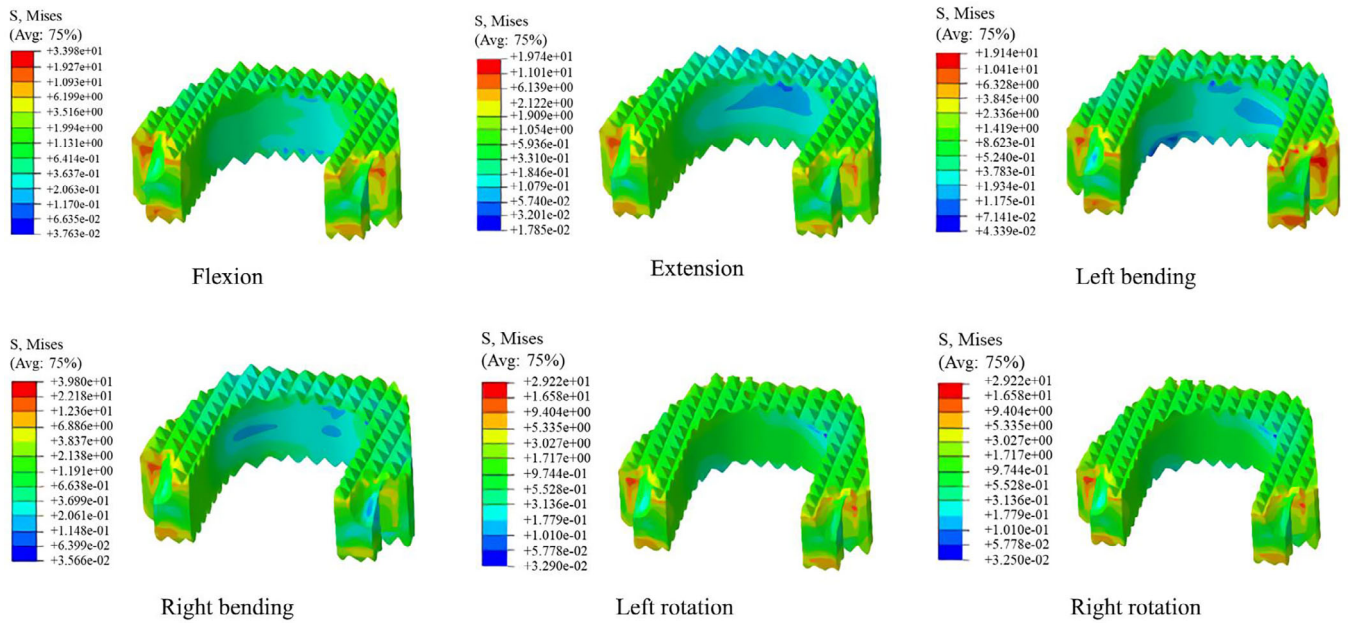


FIGURE 8 The stress distribution of interbody spacer in the “reversible kyphosis + anterior cervical discectomy and fusion” model. The maximum Von Mises stress of the interbody spacer occurred at the anterior part in different directions of movement

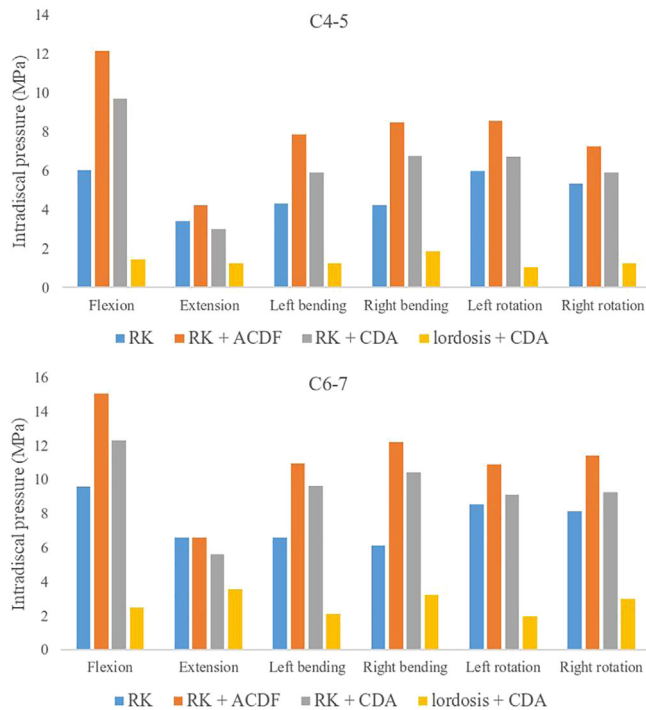


FIGURE 9 The comparison of intradiscal pressure at adjacent levels between different models

cervical spine with kyphosis were not presented.³⁶ Wei et al. reported the stress and ROMs of the straightened cervical spine rather than the kyphotic one.³⁷ Pramudita et al. reported the 100-ms relative intervertebral rotations of five head-neck FE models.³⁸

In terms of the study of John and colleagues,³⁵ they established lordotic, straight, and kyphotic FE cervical spine models

to investigate the influence of sagittal alignment on the ROM after corpectomy. Perhaps due to the unavailability of ROMs of the cervical spine with kyphosis, their segmental ROMs were validated with physiological moment-rotation characteristics reported from cadaver experiments (the cervical spine with lordosis). They also described the ROMs of the kyphotic model in flexion and extension before and after corpectomy. To our knowledge, it was the only FE study that reported the ROMs of the intact cervical spine with kyphosis. Our ROMs of RK model in extension or flexion were similar to those of John et al.³⁵

4.2 | The FE analysis of single-level CDA in the spine with lordosis or RK

This FE analysis showed that RK would decrease the ROM at surgical and adjacent levels in extension, lateral bending, and axial rotation but increase the flexion ROM. These results were in agreement with some previous studies.^{37,39} Wei et al. reported the ROM of the cervical spine with reduced lordosis decreased 24%–33% compared to that of the normal physiological model. Miyazaki et al. observed the translational motion and angular variation tended to decrease at all levels when the alignment shifted from normal to less lordotic.³⁹ However, John et al. found the flexion ROM decreased by an average of 13% with the change in sagittal alignment from lordosis to kyphosis,³⁵ which was inconsistent with our results. This contradiction could be partly explained by the different modeling methods of cervical spine. In John's study, the mesh morphing and rigid body rotation were used to generate straight and kyphotic models from the baseline lordotic model.³⁵

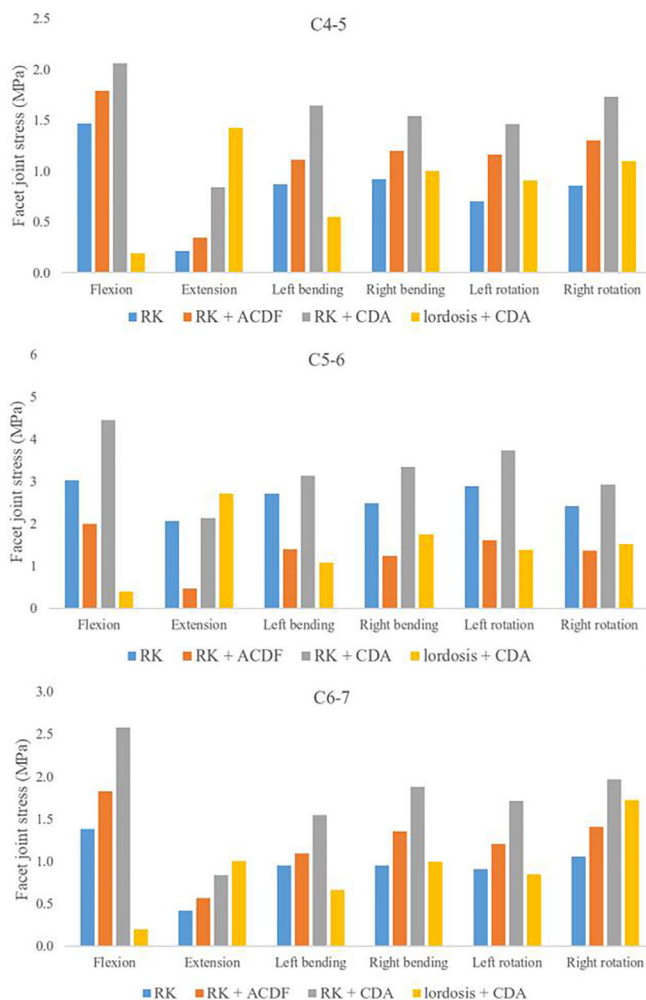


FIGURE 10 The comparison of facet joint stress between different models

This method largely neglected the compatibility, fitness, and alteration of delicate bone structures (such as facet joint and uncovertebral joint) that might experience deformation along with cervical alignment change, presumably leading to increased stiffness eventually.

This FE analysis found that RK could significantly increase the stress of anterior column (intervertebral disc at adjacent levels and Prestige LP Disc) and posterior column (facet joints). Similarly, Wei et al. reported the Von Mises stress of the cervical spine with reduced lordosis were all higher than the normal model, increasing 50%–95% under different load conditions.³⁷ It was speculated that the reduced lordosis or kyphosis of cervical spine tended to shift the greater part of the load from the posterior columns to the anterior column, which could potentially increase adjacent segment mechanical load and contribute to the development of adjacent segmental degeneration.²⁰ On the other hand, the IDP values at adjacent levels of kyphotic models were significantly higher than those of lordotic models, indicating the risk of disc rupture or herniation at adjacent levels was much higher in the cervical spine with kyphosis.

4.3 | The FE analysis of single-level CDA and ACDF in the spine with RK

This study found both CDA and ACDF increased the ROM of adjacent levels. However, compared with “RK + CDA,” the ROM of “RK + ACDF” decreased by an average of 70.47% at the surgical level and increased 4.68% and 20.3% at C4–C5 and C6–C7 levels, respectively. The FE analysis of Hua et al.,²² Choi et al.,⁴⁰ and Grandhi et al.⁴¹ reported similar results, indicating that CDA could theoretically slow down adjacent segment degeneration by preserving the intervertebral motion of implanted spine unit.

This study observed that compared with ACDF, CDA could significantly reduce the prosthesis interface stress and IDP at adjacent levels and increase the facet joint stress at the surgical levels. In this study, compared with “RK + ACDF,” the maximum prosthesis interface stress of “RK + CDA” decreased an average of 45.53%; the IDP decreased an average of 29.2% at C4–C5 level and 19.03% at C6–C7 level; the facet joint stress increased 2.69 folds in average. Likewise, Choi et al. reported that the Prodisc-C led to increased motion and facet joint stress at the index level and decreased motion, facet joint stress, and IDP at both adjacent levels.⁴⁰ In an in vitro study with cadaveric cervical specimens, Zhao et al. revealed the maximum facet joint stress of CDA was 2.72 times higher than ACDF on average.⁴² It was speculated that ACDF eliminated the intervertebral motion at the surgical level, causing the stress concentration in the anterior column at the surgical and adjacent levels. Also, the fused segments blocked the motion of facet joints, which gave rise to the stress shielding and prevented the force transmission. It should be noted that the maximum facet joint stress of “RK + CDA” was 40.3% higher than that of “RK + ACDF.” The fixed load (1 N-m moment) and increased stiffness at adjacent levels caused by ACDF could explain this result.

There are several limitations in this FE study. First, there was no muscular tissue in this cervical spine model. Thus, the FE model could not fully simulate the natural cervical spine.³⁰ Second, the surgical procedure was largely simplified in FE models. For instance, the distraction of vertebrae before inserting a prosthesis was not simulated.²¹ Third, this study only involved two kinds of prostheses. Other artificial cervical discs like Bryan Cervical Disc, Prodisc-C, and the traditional “cage + plate” procedure were not simulated. These prostheses and surgical procedures may have different materials, kinematics, and fixation methods, which might bring about diverse results.

5 | CONCLUSIONS

RK significantly changed the biomechanics of CDA, which is demonstrated by the decreased ROM and the significantly increased prosthesis interface stress, IDP, and facet joint stress in the “RK + CDA” model. Compared with ACDF, CDA overall exhibited a better biomechanical performance in the cervical spine with RK, with the increased ROM of surgical level and facet joint stress and the decreased ROM of adjacent levels, prosthesis interface stress, and IDP.

ACKNOWLEDGMENTS

This study was funded by the 1-3-5 Project for Disciplines of Excellence - Clinical Research Incubation Project, West China Hospital, Sichuan University (2019HXFH040), Chengdu Science and Technology Program Projects (2017-CY02-00025-GX), National Natural Science Foundation of China (81902190), the Science And Technology Project of The Health Planning Committee of Sichuan (21PJ039), and Key Research and Development Project of Science and Technology Department of Sichuan Province (2020YFS0084).

CONFLICT OF INTEREST

The authors declare that this research was conducted in the absence of any commercial or financial relationships that could have appeared to influence the work reported in this paper.

ORCID

Beiyu Wang  <https://orcid.org/0000-0001-8755-1427>

REFERENCES

- Carrier CS, Bono CM, Lebl DR. Evidence-based analysis of adjacent segment degeneration and disease after ACDF: a systematic review. *Spine J.* 2013;13:1370-1378.
- Nanda Anil, Sharma Mayur, Sonig Ashish, Ambekar Sudheer, Bollam Pappireddy. Surgical Complications of Anterior Cervical Discectomy and Fusion for Cervical Degenerative Disk Disease: A Single Surgeon's Experience of 1576 Patients. *World Neurosurgery.* 2014;82(6):1380-1387. <https://doi.org/10.1016/j.wneu.2013.09.022>
- Baaj AA, Uribe JS, Vale FL, Preul MC, Crawford NR. History of cervical disc arthroplasty. *Neurosurg Focus.* 2009;27:E10.
- Findlay C, Ayis S, Demetriades AK. Total disc replacement versus anterior cervical discectomy and fusion: a systematic review with meta-analysis of data from a total of 3160 patients across 14 randomized controlled trials with both short- and medium- to long-term outcomes. *Bone Joint J.* 2018;100-b:991-1001.
- Gornet MF, Burkus JK, Shaffrey ME, Schranck FW, Copay AG. Cervical disc arthroplasty: 10-year outcomes of the Prestige LP cervical disc at a single level. *J Neurosurg Spine.* 2019;31:317-325.
- Lavelle WF, Riew KD, Levi AD, Florman JE. Ten-year outcomes of cervical disc replacement with the BRYAN cervical disc: results from a prospective, randomized controlled clinical trial. *Spine (Phila Pa 1976).* 2019;44:601-608.
- Guo GM, Li J, Diao QX, et al. Cervical lordosis in asymptomatic individuals: a meta-analysis. *J Orthop Surg Res.* 2018;13:147.
- Xu H, Liu H, Hong Y, et al. Clinical and radiological outcomes of single-level cervical disc arthroplasty in the patients with preoperative reversible kyphosis: a matched cohort study. *Clin Neurol Neurosurg.* 2020;198:106247.
- Kim SW, Kim TH, Bok DH, et al. Analysis of cervical spine alignment in currently asymptomatic individuals: prevalence of kyphotic posture and its relationship with other spinopelvic parameters. *Spine J.* 2018;18:797-810.
- Sasso RC, Anderson PA, Riew KD, Heller JG. Results of cervical arthroplasty compared with anterior discectomy and fusion: four-year clinical outcomes in a prospective, randomized controlled trial. *J Bone Joint Surg Am.* 2011;93:1684-1692.
- McAfee PC, Cappuccino A, Cunningham BW, et al. Lower incidence of dysphagia with cervical arthroplasty compared with ACDF in a prospective randomized clinical trial. *J Spinal Disord Tech.* 2010;23:1-8.
- Joaquim AF, Makhni MC, Riew KD. Evidence-based use of arthroplasty in cervical degenerative disc disease. *Int Orthop.* 2019;43:767-775.
- Kani KK, Chew FS. Cervical disc arthroplasty: review and update for radiologists. *Semin Roentgenol.* 2019;54:113-123.
- Fong SY, DuPlessis SJ, Casha S, et al. Design limitations of Bryan disc arthroplasty. *Spine J.* 2006;6:233-241.
- Anakwenze OA, Auerbach JD, Milby AH, et al. Sagittal cervical alignment after cervical disc arthroplasty and anterior cervical discectomy and fusion: results of a prospective, randomized, controlled trial. *Spine (Phila Pa 1976).* 2009;34:2001-2007.
- Guérin P, Obeid I, Gille O, et al. Sagittal alignment after single cervical disc arthroplasty. *J Spinal Disord Tech.* 2012;25:10-16.
- Chen Y, He Z, Yang H, Wang X, Chen D. Clinical and radiological results of total disc replacement in the cervical spine with preoperative reducible kyphosis. *Int Orthop.* 2013;37:463-468.
- Rong X, Hu X, Liu H, Hong Y, Wang B. Cervical alignment after cervical arthroplasty with Prestige-LP Disc at C5-C6 level. *World Neurosurg.* 2020;140:e33-e40.
- Hu X, Liu H, Wang B, et al. Cervical disc arthroplasty versus anterior cervical discectomy and fusion for the treatment of single-level disc degenerative disease with preoperative reversible kyphosis. *Clin Neurol Neurosurg.* 2021;202:106493.
- Scheer JK, Tang JA, Smith JS, et al. Cervical spine alignment, sagittal deformity, and clinical implications: a review. *J Neurosurg Spine.* 2013;19:141-159.
- Wu TK, Meng Y, Liu H, et al. Biomechanical effects on the intermediate segment of noncontiguous hybrid surgery with cervical disc arthroplasty and anterior cervical discectomy and fusion: a finite element analysis. *Spine J.* 2019;19:1254-1263.
- Hua W, Zhi J, Wang B, et al. Biomechanical evaluation of adjacent segment degeneration after one- or two-level anterior cervical discectomy and fusion versus cervical disc arthroplasty: a finite element analysis. *Comput Methods Programs Biomed.* 2020;189:105352.
- Fan W, Guo LX. The effect of non-fusion dynamic stabilization on biomechanical responses of the implanted lumbar spine during whole-body vibration. *Comput Methods Programs Biomed.* 2020;192:105441.
- Li XF, Lv ZD, Yin HL, Song XX. Impact of adjacent pre-existing disc degeneration status on its biomechanics after single-level anterior cervical interbody fusion. *Comput Methods Programs Biomed.* 2021;209:106355.
- Schmidt H, Heuer F, Simon U, et al. Application of a new calibration method for a three-dimensional finite element model of a human lumbar annulus fibrosus. *Clin Biomech.* 2006;21:337-344.
- Fan R, Liu J, Liu J. Prediction of the natural frequencies of different degrees of degenerated human lumbar segments L2-L3 using dynamic finite element analysis. *Comput Methods Programs Biomed.* 2021;209:106352.
- Polikeit A, Ferguson SJ, Nolte LP, Orr TE. Factors influencing stresses in the lumbar spine after the insertion of intervertebral cages: finite element analysis. *Eur Spine J.* 2003;12:413-420.
- Denozière G, Ku DN. Biomechanical comparison between fusion of two vertebrae and implantation of an artificial intervertebral disc. *J Biomech.* 2006;39:766-775.
- Hu X, Jiang M, Liu H, et al. Five-year trends in center of rotation after single-level cervical arthroplasty with the Prestige-LP Disc. *World Neurosurg.* 2019;132:e941-e948.
- Yuan W, Zhang H, Zhou X, Wu W, Zhu Y. The influence of artificial cervical disc prosthesis height on the cervical biomechanics: a finite element study. *World Neurosurg.* 2018;113:e490-e498.
- Galbusera F, Bellini CM, Costa F, Assietti R, Fornari M. Anterior cervical fusion: a biomechanical comparison of 4 techniques. Laboratory investigation. *J Neurosurg Spine.* 2008;9:444-449.
- Panjabi MM, Crisco JJ, Vasavada A, et al. Mechanical properties of the human cervical spine as shown by three-dimensional load-displacement curves. *Spine (Phila Pa 1976).* 2001;26:2692-2700.
- Ito S, Ivancic PC, Panjabi MM, Cunningham BW. Soft tissue injury threshold during simulated whiplash: a biomechanical investigation. *Spine (Phila Pa 1976).* 2004;29:979-987.

34. Liu Q, Guo Q, Yang J, et al. Subaxial cervical intradiscal pressure and segmental kinematics following atlantoaxial fixation in different angles. *World Neurosurg.* 2016;87:521-528.
35. John JD, Kumar GS, Yoganandan N, Rajshekhar V. Influence of cervical spine sagittal alignment on range of motion after corpectomy: a finite element study. *Acta Neurochir.* 2021;163:251-257.
36. Chen WM, Jin J, Park T, Ryu KS, Lee SJ. Strain behavior of malaligned cervical spine implanted with metal-on-polyethylene, metal-on-metal, and elastomeric artificial disc prostheses - a finite element analysis. *Clin Biomech (Bristol, Avon).* 2018;59:19-26.
37. Wei W, Liao S, Shi S, Fei J, Wang Y, Chen C. Straightened cervical lordosis causes stress concentration: a finite element model study. *Australas Phys Eng Sci Med.* 2013;36:27-33.
38. Pramudita Jonas A., Kikuchi Shunsuke, Minato Izumi, Tanabe Yuji. Effect of cervical spine alignment on neck injury risk during rear-end impact - numerical study using neck finite element model. *International Journal of Crashworthiness.* 2017;22:(4):453-466. <https://doi.org/10.1080/13588265.2017.1278638>
39. Miyazaki M, Hymanson HJ, Morishita Y, et al. Kinematic analysis of the relationship between sagittal alignment and disc degeneration in the cervical spine. *Spine (Phila Pa 1976).* 2008;33:E870-E876.
40. Choi H, Purushothaman Y, Baisden JL, Rajasekaran D, Jebaseelan D, Yoganandan N. Comparative finite element modeling study of anterior cervical arthrodesis versus cervical arthroplasty with Bryan disc or Prodisc C. *Mil Med.* 2021;186:737-744.
41. Gandhi AA, Grosland NM, Kallemeyn NA, et al. Biomechanical analysis of the cervical spine following disc degeneration, disc fusion, and disc replacement: a finite element study. *Int J Spine Surg.* 2019;13:491-500.
42. Zhao X, Yuan W. Biomechanical analysis of cervical range of motion and facet contact force after a novel artificial cervical disc replacement. *Am J Transl Res.* 2019;11:3109-3115.

How to cite this article: Hu, X., Jiang, M., Hong, Y., Rong, X., Huang, K., Liu, H., Pu, D., & Wang, B. (2022). Single-level cervical disc arthroplasty in the spine with reversible kyphosis: A finite element study. *JOR Spine*, 5(2), e1194. <https://doi.org/10.1002/jsp2.1194>